ECI Symposium Series, Volume RP5: Proceedings of 7th International Conference on Heat Exchanger Fouling and Cleaning - Challenges and Opportunities, Editors Hans Müller-Steinhagen, M. Reza Malayeri, and A. Paul Watkinson, Engineering Conferences International, Tomar, Portugal, July 1 - 6, 2007

EXPERIMENTAL INVESTIGATION OF CRYSTALLIZATION FOULING ON GROOVED STAINLESS STEEL SURFACES DURING CONVECTIVE HEAT TRANSFER

A. Al-Janabi[1], M.R. Malayeri[1] and H. Müller-Steinhagen[1,2]

[1] Institute for Thermodynamics and Thermal Engineering (ITW), University of Stuttgart
Pfaffenwaldring 6, D-70550, Stuttgart, Germany, herz@itw.uni-stuttgart.de
[2] Institute for Technical Thermodynamics, German Aerospace Centre (DLR), Pfaffenwaldring 38-40,
D-70569, Stuttgart, Germany

ABSTRACT

The beneficial aspects of enhanced or extended heat transfer surfaces may be off-set if operated under fouling conditions. In the present paper, preliminary experimental results for crystallization fouling of $CaSO_4$ solutions onto surfaces with different structures are reported. Flat stainless steel plates (50 mm x 59 mm) with 'V' shaped grooves on the side of fluid flow were used as heat transfer surfaces. Experiments were carried out both under clean and fouling conditions to discern how the same surface structures perform under such circumstances. In addition, the impact of both, the direction of grooves with respect to fluid flow (crossed, longitudinal and mixed flow grooves) and the groove dimensions has also been investigated. Fouling trends are discussed in terms of delay time and fouling rate. Significant differences have been found for the various flow conditions.

INTRODUCTION

Alteration of surfaces geometry is one of the techniques to enhance heat transfer in heat exchangers, resulting in increased contact surface area as well as stronger agitation of the boundary layer. Among the more well-known examples are fins or grooves that behave as disturbance promoters by increasing fluid mixing and extending heated surface area. Thus, such techniques are frequently exploited to manufacture more compact and smaller heat exchangers with higher efficiency.

Over the past decades tremendous efforts have been devoted to better understanding of flow mixing and heat transfer enhancement in channels with different geometries, like grooved, wavy and corrugated channels (Ghaddar et al., 1986; Greiner, 1991; Wang and Vanka, 1995). Of these, grooved channels are utilized in wide range of industrial and biomedical applications. Wu et al. (2002) showed that grooves on aluminium heat transfer surfaces lowered the cooling water flow resistance and enhanced the heat transfer coefficients by up to 2-3 times as compared to those of flat plates. While excellent performance is often reported for compact heat exchangers under clean conditions, opposite trends were observed when subjected to fouling, since the to narrow channels are readily plugged by deposits. No fundamental study has been undertaken so far to investigate how the surface structure in form of structured small grooves (size, shape, and direction to the flow) may influence crystallization fouling behaviour. Previous studies are restricted to the fouling of micro heat exchangers. Heinzel et al. (2007) investigated particulate fouling of rectangular channels with typical widths of 100-200 μm using a μPIV (micro Particle Imaging Velocimetry) technique. They showed that most of the particulate deposition occurs on the edges of the channels as well as at the inlet grid wall of micro heat exchangers. In addition, Benzinger et al. (2005) studied the precipitation of calcium carbonate within micro-channels under the influence of ultrasound as means of deposition removal. They showed that the operating time of micro heat exchangers without or with less deposits could be extended using ultrasound.

The purpose of the present study is to investigate crystallization fouling characteristics for turbulent flows over grooves on stainless steel surfaces. 'V' shaped grooves with an angle of 90° have been investigated under both clean and fouling conditions with different dimensions with respect to depth and width. Fouling experiments have been carried out with calcium sulphate as a foulant for a given bulk temperature and bulk concentration, respectively.

EXPERIMENTATION AND PROCEDURE

Solution Preparation and Measurement

Calcium sulphate: The working solution of $CaSO_4$ is prepared by directly dissolving calcium nitrate tetra-hydrate, $Ca(NO_3)_2.4H_2O$, and sodium sulphate, Na_2SO_4 in distilled water as per Equation (1). The two chemicals were initially dissolved separately in 23.5 litres of distilled water and mixed together in a 60 litre stainless steel vessel in such a way that the desired $CaSO_4$ concentration is finally achieved.

$$Ca(NO_3)_2.4H_2O + Na_2SO_4 \rightarrow CaSO_4 + 2NaNO_3 + 4H_2O \quad (1)$$

Concentration measurement. Solution concentration can be determined by measuring the calcium ion concentration by potentiometric EDTA titration (Fritz and

Produced by The Berkeley Electronic Press, 2016

Schenk, 1987). The titrant (H_2Y^{2-}) is a solution of the disodium salt of EDTA (disodium dihydrogen ethylene-diamine-tetra-acetate) In order to clearly distinguish the end point of titration, a certain amount of magnesium sulphate ($MgSO_4$) was also used as indicator. Magnesium sulphate has to have the same concentration of titrant (H_2Y^{-2}) which was of 0.01 mol/L, so the added amount of magnesium was subtracted from the total EDTA consumption. Finally, the pH value of the titration sample was adjusted to a value of 9-10 by adding 2-3 ml of ammonia buffer solution with pH=10. The stoichiometric reaction is as follows:

$$\left(Ca + Indic^{-}\right) + H_2Y^{2-} \rightarrow CaY^{2-} + H\,Indic^{2-} + H^{+} \qquad (2)$$

Surface Characterization

Heat transfer surfaces. The heated surfaces were all of basic material stainless steel AISI 304 BA (50 x 59 mm) with a wall thickness of 0.3 mm.

Roughness measurement. Before making the grooves, a stylus instrument (Perthometer M4Pi, Mahr, Germany), as illustrated in Figure 1, was used to measure the base surface roughness of the samples over a length of 15 mm in three horizontal and vertical lines.

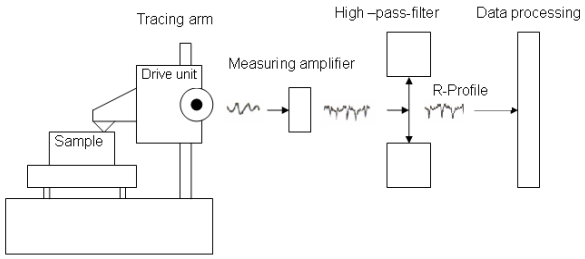

Fig. 1 Experimental arrangement of the stylus device.

The mean values of different roughness profiles such as R_a, arithmetic mean value R_z and the root mean square value of the heat surfaces are then determined, as listed in Table 1, by taking the mean points of the intersection between the horizontal and vertical lines, as shown in Figure 2.

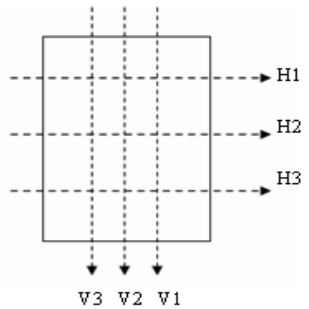

Fig. 2 Positions and directions of surface roughness measurements.

Table 1 Characteristics of surface roughness

Direction	R_a µm	R_q µm	R_z µm
H1	0.49	0.62	2.72
H2	0.54	0.7	4.94
H3	0.56	0.73	5.1
V1	0.54	0.69	4.79
V2	0.46	0.59	3.23
V3	0.59	0.76	5.0
Average of intersection	0.53	0.68	4.29

Surface structure: The categorisation of different surface structures used in this study is shown in Figure 3. Grooves are classified into 1) groove shapes in "V" form or rectangular grooves; 2) groove dimensions in terms of width and depth; and 3) groove direction with respect to the direction of fluid flow which are crossed, longitudinal, and mixed direction grooves. In the present paper, however, only the results of "V" shaped grooves will be presented as only a few and yet non-conclusive results have been obtained for the latter surfaces. 2D and 3D sketches of "V" shaped grooves in terms of dimension and direction are illustrated in Figures 4-7.

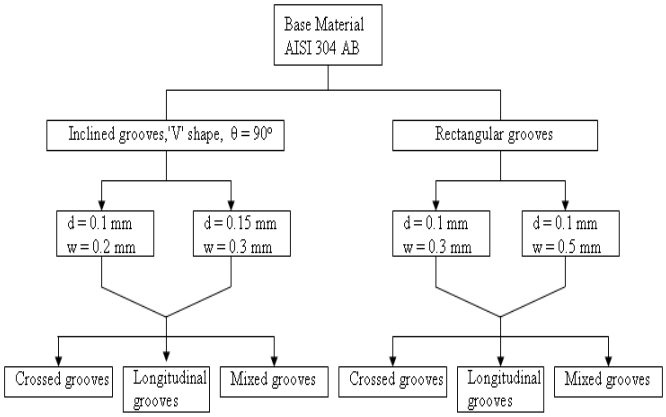

Fig. 3 Flowchart of different grooved surfaces.

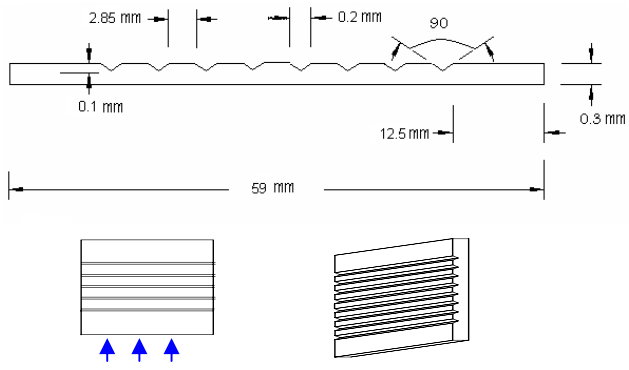

Fig. 4 Crossed grooves (θ = 90°, d = 0.1 mm, and w = 0.2 mm).

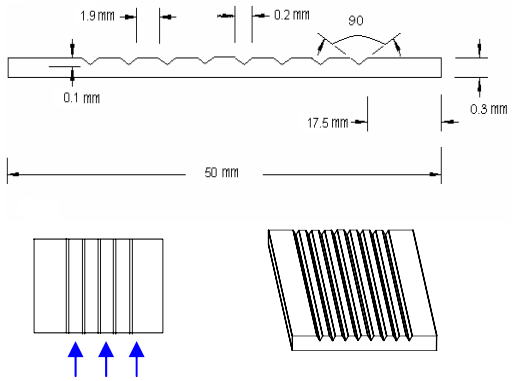

Fig. 5 Longitudinal grooves (θ = 90°, d = 0.1 mm, and w = 0.2 mm).

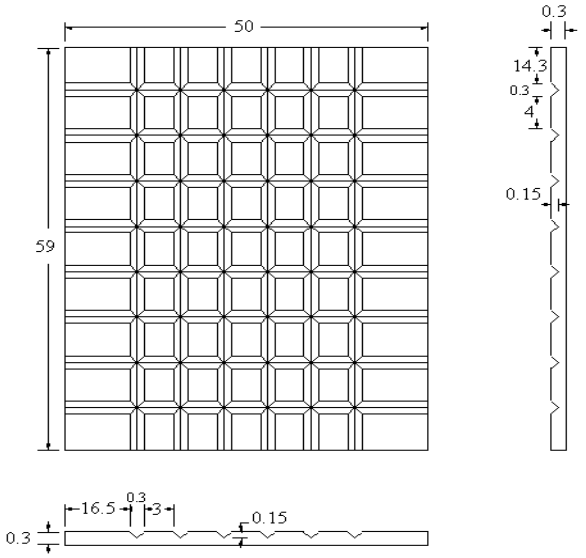

Fig. 6 Mixed grooves with (d = 0.15 mm, and w = 0.3 mm).

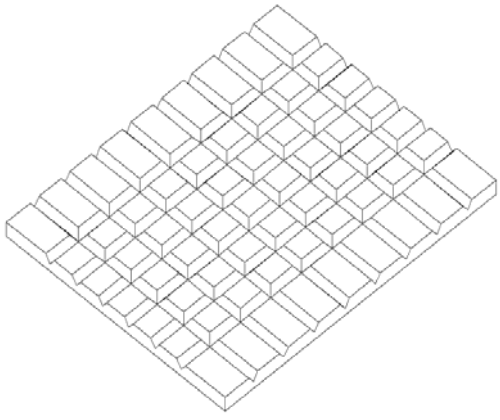

Fig. 7 3D of surfaces with "V" shaped mixed grooves.

EXPERIMENTAL RIG AND DATA ACQUISITION

The test rig, as depicted in Figure 8, consists of a closed-flow loop in which the calcium sulphate solution is continuously re-circulated from a stainless steel supply tank through a 12 μm filter and heated test sections. The filter is used to remove broken crystals and other impurities from the solution. A bypass pipe system leading from the pump back to the tank was installed to avoid pump damage and to have better flow control. Each test section is a vertical rectangular duct with a dimension of (39mm x 13mm x1670 mm length) and contains two parallel plate surfaces of the same dimensions which are connected to an adjustable power supply.

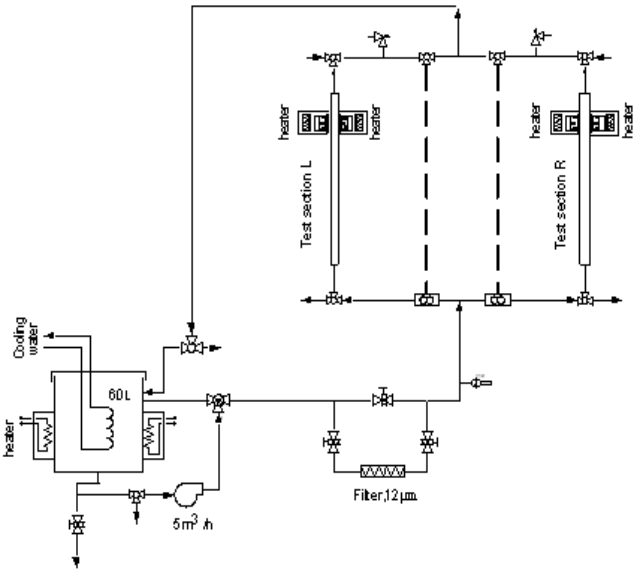

Fig. 8 Schematic diagram of the experimental set-up

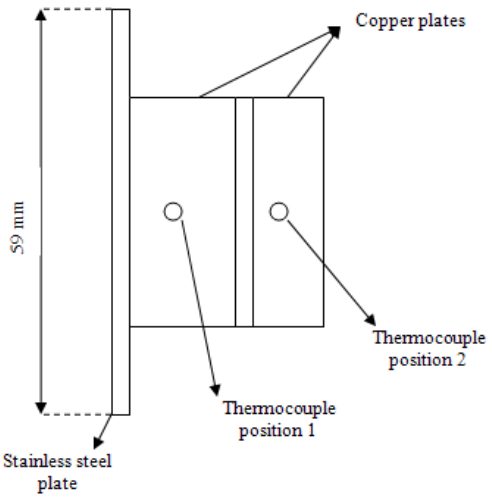

Fig. 9 2D sketch of the heat transfer surface

During all experiments, the heat flux is kept constant by using a closed loop controller with an electronic dimmer. The surface temperature is measured with K-type (Ni-Cr / Ni-Al) thermocouples mounted in the copper plates as shown in Figure 9. A second thermocouple is also placed in the same copper plates with a distance of 12.5 mm from the first one in order to determine the heat flux.

A computer controlled data acquisition system is used to log and process all experimental data such as solution flow rate, bulk temperature, heat flux, cooling water temperature and the surface temperature. The analysis of the measured data takes place on a separate PC using MS Excel.

EXPERIMENTAL PROCEDURES FOR CLEAN AND FOULING RUNS

Before mounting the surfaces into the test rig, they were cleaned with toluene to remove any contaminations. The test rig is then run with distilled water until the surface temperature became stable for more than one hour.

For clean conditions the recording was then initiated; for fouling runs, the water was then removed and replaced by calcium sulphate solution. After another ten minutes, the heating is switched on and the data collection started. The temperature of the solution in the supply tank is regulated by an adjustable water-cooled coil inside the tank, together with two heater pads installed on the outer surface of the tank. The solution is then fed from a 60 litre stainless steel supply tank to the test section by a centrifugal pump. The flow rate can be adjusted by valves and continuously measured with a flow meter.

RESULTS AND DISCUSSION

Heat Transfer over Grooved Surfaces

Heat transfer within grooves is more complex than that on flat plates. This is due to substantial turbulence caused by the eddies generated within the channels which, in turn, depend on the groove dimensions and their direction to the flow. Therefore, before presenting heat transfer coefficients under both clean and fouling conditions, it is indispensable to discern how the flow field changes as a result of different surface structures and also under which circumstances heat transfer surfaces may perform better.

As fluid flows over crossed grooves, eddies whose vortexes are opposite to those of the mainstream flow are generated that will cause an adverse pressure gradient. Consequently, the generation of eddies in the groove itself may lead to strong mixing and subsequently further agitation of the boundary layer. Another effect is due to the plume emission at the corner of the grooves as shown in Figure 10. These plumes can be generated in the shape of either backward or rotating eddies when there is abrupt change in the surface texture as shown in this figure. Less eddies are expected for flow over mixed grooves and, even more so, for longitudinal grooves. These hypotheses are consistent with the findings of Chen et al. (2006), who showed that no additional pressure drag was generated in longitudinal grooves while the crossed grooves caused stronger drag forces.

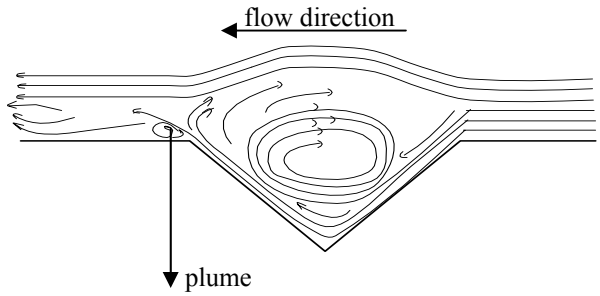

Fig. 10 Streamlines for a turbulent flow over crossed grooves.

Clean Heat Transfer Coefficient

Several experiments have been carried out to determine the effect of flow velocity on the clean heat transfer coefficient during convective heat transfer. As expected, as the velocity increases the heat transfer coefficient also improves for all different groove geometries, regardless of their dimensions and directions to flow.

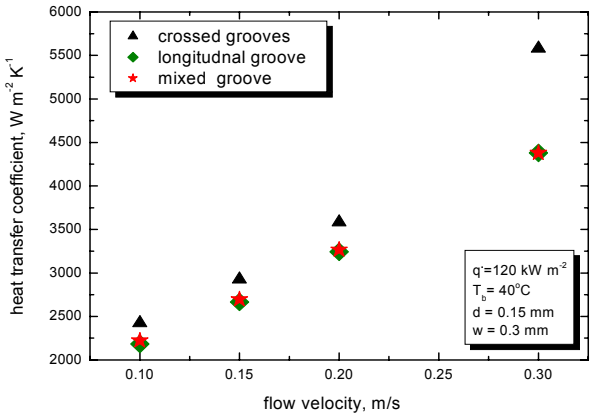

Fig. 11 Effect of flow velocity on the heat transfer coefficient of 'V' grooved surfaces.

The main reason for this effect is the increasing turbulence level of the bulk flow which, in turn, leads to a higher degree of turbulence within the grooves. Such trends are clearly evident in Figure 11 for a given heat flux of 120 kW/m^2. A higher heat transfer coefficient was observed for crossed grooves in comparison to longitudinal and mixed grooves, which both exhibit almost the same heat transfer coefficients as velocity varies.

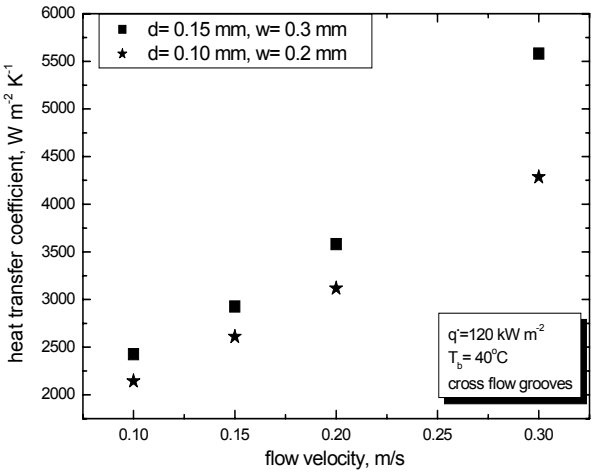

Fig. 12 Variation of heat transfer coefficient with velocity over crossed grooves with different dimensions.

The groove dimensions (width and depth) have a significant influence on the heat transfer coefficient as shown in Figure 12. Increasing the groove width by only 0.1 mm resulted in 10% higher heat transfer coefficients for lower velocities and up to 25% higher values for higher velocities. This may be the result of more and larger eddies and consequently higher level of mixing flow that is expected in grooves with larger dimensions of and vice versa for smaller and narrower grooves.

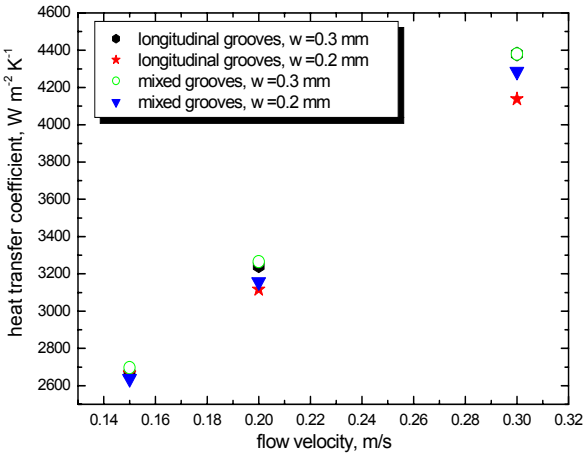

Fig. 13 Heat transfer coefficient versus velocity for longitudinal and mixed grooves.

These findings are in good agreement with the results reported by Wang (2003). He showed that the flow in narrow grooves is quite different from that in wide grooves, since the streamlines do not produce eddies or plumes. Moreover, Wu et al. (2002) confirmed the observations that the Nusselt number increases with increasing groove depth.

The impact of groove dimensions is only marginal for the two other structures. Figure 13 depicts that while the flow velocity increases over longitudinal and mixed grooved surfaces the differences between the two heat transfer coefficients are negligible, particularly for lower flow velocities. This is a result of the generated streamlines around longitudinal and mixed grooves, which do not show any resistance to the flow as this was the case for the crossed grooves (Wu et al., 2002). For higher velocities, however, it can be concluded that the magnitude of turbulence may depend more upon the surface structure, resulting in higher heat transfer coefficients for the larger dimensions.

Heat Transfer Coefficients under Fouling Conditions

Surface structures with different shapes, dimensions, and directions may also be of interest when subjected to fouling. This is because, under fouling conditions, the generated eddies and plumes, as shown in Figure 10, may give rise to substantially stronger drag forces that may overcome the adhesion forces between the growing crystals and the surface, and consequently lead to shearing-off of the early deposit. For longitudinal grooves, a smaller flow resistance is anticipated and thus crystal nuclei are less likely to spall off the surface.

Figure 14 shows that the induction time (the initial time that elapses before fouling deposition becomes noticeable) is a strong function of the groove direction with respect to the fluid flow. Longer induction times occurred over the crossed grooves in comparison with longitudinal and mixed grooves. As stated before, the crossed grooves have a higher resistance to the flow than the other two surface textures, and hence provide a stronger inhibition to the formation of initial nuclei.

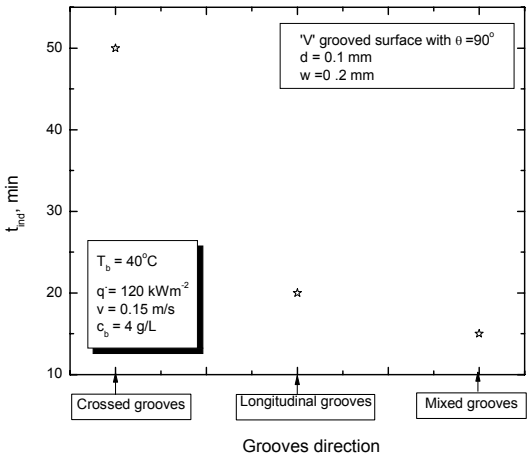

Fig. 14 Induction time as a function of groove direction.

Increasing the groove dimensions has a positive impact on the induction time as shown in Figure 15. This figure presents a comparison between two longitudinally grooved surfaces for a constant heat flux of 120 kW/m^2 for variable groove depth and width. Increasing the depth of grooves led to a longer induction time but there is no significant reduction in the fouling resistance during the first 160 minutes. However, after this time, the fouling curves level off but still progress but with much smaller slope. This implies that once the surface is covered by an initial layer of deposit, the dependence of the fouling process on the groove dimensions will be reduced.

Similar results are shown in Figure 16 but for the crossed grooves. For better comparison between the various dimensions, the fouling rates (i.e. the initial slopes of the fouling curves) are determined and shown in this figure. It is evident that an increase in both depth and width of grooves causes a significant reduction of fouling rate from 1.53×10^{-4} to 1.045×10^{-4} (m^{2}K/kJ). No such trend was seen for longitudinal grooves, where both dimensions exhibit the same fouling rate (see Figure 15). The reduction in fouling rate can be attributed to a high level of mixing within the grooves due to the entrapped eddies inside larger cavities. The same eddies may sweep away initial crystal nuclei which attempt to form inside the grooves. Asymptotic fouling resistance was also observed to prolong for larger dimensions of grooves and vice versa for smaller dimensions.

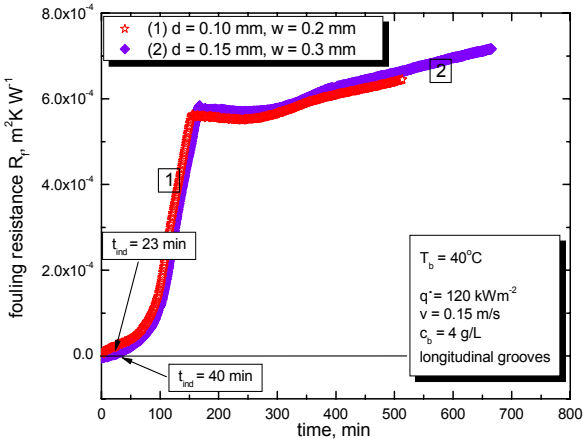

Fig. 15 Fouling resistance versus time for longitudinal grooves with variable dimensions.

Figure 17 presents three pictures of deposit layers on different surface structures for the same dimensions and operating conditions. Visual examination of these fouled surfaces after each run indicates that crossed grooves have a fragile and thin deposit layer, while for longitudinal and mixed grooves the fouling layer was relatively thick and adhesive.

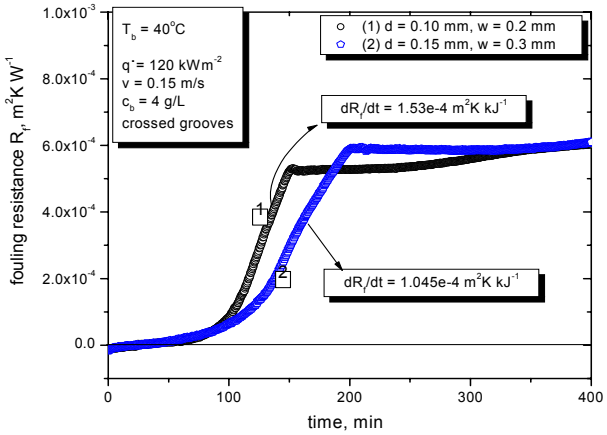

Fig. 16 Fouling resistance versus time for crossed grooves with variable dimensions.

The impact of entrapped eddies is also evident inside the crossed grooves, in which either no or only little deposit was observed, see Figure 17-a. Contrariwise, a homogenous deposit layer is evident for the other two structures. More analyses are required to examine surface morphology and crystals that are formed on each surface.

a) Crossed grooves

b) Longitudinal grooves

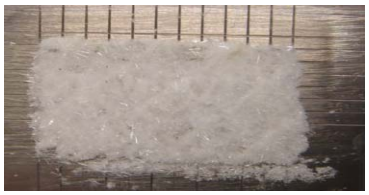

c) Mixed grooves

Fig. 17 Fouling layer on 'V' grooved surfaces with d = 0.1 mm, and w = 0.2 mm for T_b = 40°C, v = 0.15 m/s, q˙ = 120 kW/m^2 and c_b= 4 g/L.

CONCLUDING REMARKS

The following conclusions can be drawn from the experimental results of this study:

1. Clean heat transfer coefficients increased with velocity for all investigated groove directions, but mostly for the crossed ones.
2. Crossed grooves intensify the clean heat transfer as both the depth and width are increased. No significant impact of dimensions was observed for longitudinal and mixed grooves.
3. Of all three different surface structures, the least deposition occurred for the crossed grooves. Higher flow resistance and hence stronger drag forces are anticipated for crossed flow which may assist in removal of initial crystals forming on the surface.
4. For longitudinal and mixed structures, while no substantial changes in clean heat transfer coefficient were seen for various dimensions, longer induction times were observed for larger dimensions. However, variation of the dimensions did not affect the fouling rate. Contrariwise for the crossed grooves, larger dimensions gave rise to both prolongation of induction time and lower fouling rates. If any deposit layer was formed for the crossed grooves, it was more fragile and thinner than that on the other surface structures.
5. It can finally be concluded that from the three examined surface structures, the crossed grooves performed best with respect to heat transfer and fouling. This will have to be assessed against the associated increase in pressure drop.

NOMENCLATURE

c Concentration, g/L
d Depth of groove, m
$\dot{q}$ Heat flux, kW/m^2
R_f Fouling resistance, m^2 K W^{-1}
t_{ind} Induction time, min
T Temperature, ^{o}C
v Velocity, m/s
w Width of groove, mm

Subscript

b bulk

ACKNOWLEDGEMENT

The authors gratefully acknowledge the financial support of the MEDESOL Project (The European Commission, Contract no. 036986) and of the German Research Council (DFG). The first author is also indebted to the DAAD, "German Academic Exchange Service" for a research studentship.

REFERENCES

Benzinger, W., Schygulla, U., Jäger, M., and Schubert, K., 2005, Anti fouling investigations with ultrasound in a micro-structured heat exchanger. *Proc. 6th Int. Heat Exchanger Fouling and Cleaning - Challenges and Opportunities*, Kloster Irsee, Germany, Vol. RP2, pp. 197-201.

Chen, H., Chen, D., and Li, Y., 2006, Investigation on effect of surface roughness pattern to drag force reduction using rotary rheometer. *Journal of Tribology*, Vol.128, pp. 131-138.

Fritz, J.S., and Schenk, G.H., 1987, *Quantitative analytical chemistry*, 5th edition, Allyn and Bacon Inc., U.S.A

Ghaddar, N.K., Korczak, K., Mikic, B.B., and Patera, A.T., 1986, Numerical investigation of incompressible flow in grooved channels, *J. Fluid Mech*., Vol. 163, pp. 99-127.

Greiner, M., 1991, An experimental investigation of resistant heat transfer enhancement in grooved channels, *Int. J. Heat Mass Transfer*, Vol. 34, pp. 1381-1391.

Heinzel, V., Jianu, A. and Sauter, H., 2007, Strategies against particle fouling in the channels of a micro heat exchanger when performing μPIV flow pattern measurements, *J. Heat Transfer Engineering*, Vol. 28, pp. 222-229.

Wang, C.Y., 2003, Flow over a surface with parallel grooves, *Physics of Fluids*, Vol. 15, pp. 1114-1121.

Wang, G., and Vanka, S.P., 1995, Convective heat transfer on periodic wavy passages, *Int. J. Heat Mass Transfer*, Vol. 38, pp. 3219-3230.

Wu, W., Du, J.H., Ma, B., and Wang, B.X., 2002, Grooved wall effect on forced convective heat transfer in a packed channels between two parallel plates, *J. Enhanced Heat Transfer*, Vol. 9, pp. 117-121.